Near-edge x-ray-absorption fine structure of Pb: A comparison of theory and experiment

M. Newville and P. Līviņš
Department of Physics, FM-15, University of Washington, Seattle, Washington 98195

Y. Yacoby
Racah Institute of Physics, Hebrew University, Jerusalem, Israel

J. J. Rehr and E. A. Stern
Department of Physics, FM-15, University of Washington, Seattle, Washington 98195
(Received 3 August 1992; revised manuscript received 9 December 1992)

Two independent techniques are used to obtain the background function for the x-ray-absorption fine structure (XAFS) of pure Pb at energies that are normally inaccessible because they are in the edge. The results of the two techniques are shown to give the same $\chi(k)$ above a threshold energy in the absorption edge, where the background is 70% of the edge step. The reliability of the XAFS starting at unprecedentedly low k values (1.5 Å^{-1} above the Fermi energy) allows sensitive tests of several details of theoretical XAFS calculations. Electron-hole-excitation losses in addition to the plasmon-pole loss term are shown to be important, and the Hedin-Lundqvist many-body self-energy is found to be superior to that of Dirac-Hara for pure Pb. One of the presented methods of background removal can be employed for general XAFS analysis, and is easily automated.

I. INTRODUCTION

In order to get structural information from x-ray-absorption fine-structure (XAFS) data,[1] it is first necessary to separate the XAFS, χ, from the measured absorption, $\mu(E)$, according to

$$\chi(E) = \frac{\mu(E) - \mu_0(E)}{\mu_0(E)}, \tag{1}$$

where $\mu_0(E)$ is the absorption of an "isolated" atom. This is the absorption from an atom embedded in the electronic environment of the condensed system, but without backscattering from the near neighbors, and is, in general, different from the atom in a vacuum.[2] This absorption of the isolated embedded atom is not usually known, and is assumed to be a much more smoothly varying function of energy away from the absorption edge than is the XAFS. The separation of $\mu(E)$ consists of three steps:[3] (1) Pre-edge background removal, in which most of the energy dependence of the absorption other than that from the absorption edge of interest is eliminated, (2) normalization to the edge jump, and (3) post-edge background removal, in which a smoothly varying background function which approximates the absorption from the isolated embedded atom, $\mu_0(E)$, is subtracted from $\mu(E)$ to give $\chi(E)$. While the first two steps are important, they are also usually straightforward and trouble free. Pre-edge background removal will be done in the standard way, and without further comment. Normalization will be discussed briefly below.

Extracting the post-edge background function, $\mu_0(E)$, is the most critical step of background removal, as this function can affect the final conclusions for the structural information. In particular, when the variations of the background function are comparable to the XAFS itself, the separation of the background and XAFS becomes poorly defined. Since the atomic absorption varies substantially near the absorption edge, the standard practice in XAFS analysis has been to ignore everything below an energy typically 30 eV above the Fermi energy, E_F. This can be a severe limitation on the range of useful data, especially for highly disordered systems, for which the XAFS signal drops into the noise within a hundred eV from the edge.

In this paper a general method for extracting the post-edge background from experimental data, even within the absorption edge, is presented. It is more objective and reliable than previous methods and is easily automated. The new method is applied to pure Pb, and a comparison is made between the results from this method and a measured background, obtained by an independent technique[4] that finds points on the true background function. The results for the two backgrounds are shown to be essentially the same in those cases for which the measured background technique is valid. The agreement of the two independent results, even within the absorption edge, allows for a critical evaluation of theoretical calculations in this previously untested region, where the approximations used in the calculations are most suspect.

II. REVIEW OF POST-EDGE BACKGROUND METHODS

Because the absorption of an isolated embedded atom is not generally known to sufficient accuracy, and be-

cause the measured absorption can include significant, if smooth, deviations from the true absorption, the post-edge background function must be approximated. The usual practice has been to approximate the background function by a piecewise polynomial, or spline. Splines are used because they are easily calculated and can be made sufficiently flexible for nearly all situations. The flexibility of the spline is controlled by the number of knots, points along the spline at which two polynomials pieces join, and at which some discontinuity in derivatives is allowed. By using splines, the problem of how best to approximate the background is reduced to a problem of what conditions, such as polynomial order and knot location, to put on the spline.

The standard method for spline background approximation[3] is to use cubic splines, which are fourth-order polynomials with knots which have one degree of freedom each. For such cubic splines, the value of the spline and its first two derivatives are required to be continuous at the knots, while the third derivative is allowed to be discontinuous. The cubic spline is usually chosen so as to give a least-squares fit to the full absorption data, $\mu(E)$. In order to prevent the cubic spline from following the absorption spectra too closely, thereby erasing the XAFS, it is constrained to have a small number of knots. Typically between 2 and 7 knots are used. While this type of background approximation is generally successful for Extended XAFS analysis, it suffers from problems due to subjectivity in the selection of knot locations. More importantly, this method often becomes unreliable near the absorption edge, where the background varies rapidly.

An important improvement to this method of choosing a fairly stiff spline which gives the least-squares fit to the full absorption data was made by Cook and Sayers,[5] who recognized that the background corresponds to the low-R components of $\tilde{\chi}(R)$, the Fourier transform of $\chi(k)$ resulting from the background subtraction. They proposed that a good background removal would eliminate all low-R components of $\tilde{\chi}(R)$ that would distort the XAFS information, but preserve all XAFS information with sufficiently high R. The method they used to accomplish this was to start with the background function as the absorption data, and smooth this background using cubic splines through all data points until the second derivative of the background was small compared to that of the absorption data. The smoothing was then continued until the low-R magnitude of $\tilde{\chi}(R)$ was sufficiently smaller than the first peak magnitude of $\tilde{\chi}(R)$. The new background method we will introduce in the next section comes from a refinement of the proposed criteria of Cook and Sayers for a good background removal, and uses a more straightforward technique.

Recently, a method of experimentally determining the background in the near-edge region has been demonstrated. This method relies on the assumption that, while the XAFS is temperature dependent, the background is not. By measuring $\mu(E)$ at various temperatures for pure Pb between 10 and 600 K, Stern *et al.*[4] found points where the spectra of different temperatures crossed one another. These "data crossings" gave points on the background curve itself for the near-edge region, and the usual polynomial spline could then be constrained to go through these points on the known background curve. By allowing this constrained spline to best fit the absorption data, the isolated embedded atom absorption, $\mu_0(E)$, and therefore the XAFS, were quite accurately determined starting at about 8 eV above the Fermi energy, E_F (in this paper, all energies and k values will be referenced to E_F), a substantial improvement on the lower limit of energy for useful $\chi(k)$.

Although the data-crossing method is quite reliable for Pb at high temperatures, it fails when the near-edge absorption has significant contributions from more than one shell or from multiple scattering. This failure, unfortunately, disqualifies the data-crossing method for most XAFS problems of interest. The technique works in Pb because of the low Einstein temperature ($\theta_E = 66$ K) so that higher shells have large Debye-Waller factors and do not contribute to the near-edge XAFS at room temperature and above. The low Einstein temperature also implies that the thermal disorder for the first shell varies significantly at low k between room temperature and the melting temperature, allowing the data crossings to be discernible. The data-crossing technique requires XAFS measurements over a temperature range for which higher shells are negligible and the first shell Debye-Waller factor changes significantly. Even when possible, the number of different experimental measurements necessary for this method implies time-consuming data collection and analysis in many cases of interest for which they are otherwise unnecessary. A simpler, more general approach of obtaining a reliable background is desirable.

III. BACKGROUND-REMOVAL METHOD

The background-removal method presented in this paper stresses the information content of the XAFS. Because the goal of most XAFS analyses is to get structural information about the system (through the partial pair correlation function), the background function can be defined as that part of measured absorption that does not contain any structural information. This definition, similar to that of Cook and Sayers,[5] suggests an approach to its removal. Since the partial pair-correlation function is small below the first-neighbor distance, the XAFS signal must be small at low R. A correctly subtracted background function will therefore result in only small signals in the low-R part of $\tilde{\chi}(R)$. The remaining low-R components of $\tilde{\chi}(R)$ will be dominated by leakage from the first shell. Although low-frequency structure in the atomic absorption due to resonant scattering from the electronic states within the central atom have been suggested[2] and observed,[6] these are not part of the structural information sought after in most XAFS experiments. These nonstructural contributions to the total absorption are considered to be part of the background, and the new approach will separate them from the XAFS, and may give a useful way to study these electronic states.

The method we suggest is to subtract a spline that best eliminates the nonstructural, low-R, portion of $\tilde{\chi}(R)$. Since the criterion for the background is best expressed in R space, the background spline is allowed to vary un-

til the resulting $\tilde{\chi}(R)$ is optimized at low R. We will discuss the meaning of this optimization more precisely below, but it amounts to minimizing those parts of $\tilde{\chi}(R)$ at low R that do not result from leakage of the first shell. The spline used to approximate the background is a fourth-order polynomial spline with knots that are equally spaced in k space, and at which one degree of freedom in the spline is allowed. No points on the absorption curve are assumed to be points on the background curve in this method. Specifically, the spline does not necessarily intercept the absorption curve at the knots; the ordinates of the spline at the knots are determined by the low-R fit. Whereas previous methods of background removal chose a smooth spline to best fit the whole absorption spectrum, $\mu(E)$, the method chooses the spline to best fit only the low-frequency components of $\mu(E)$.

The optimization of $\tilde{\chi}(R)$ at low R for the background subtraction can be done in a two ways. The simplest way is to minimize the $\tilde{\chi}(R)$ over a low-R range in which the XAFS is known to be small. While this simple minimization is certainly an improvement over fitting the background spline in k space, it has difficulty when leakage from the first shell, due to the finite window in the Fourier transform as well as the k dependence of the backscattering, causes substantial low-R components of $\tilde{\chi}(R)$. A better optimization of $\tilde{\chi}(R)$, which will compensate for this spectral leakage, is to minimize the difference of the data $\tilde{\chi}(R)$ and a standard $\tilde{\chi}(R)$ over the low-R region. The standard $\tilde{\chi}(R)$ is used to give an estimate of the leakage into the low-R region from the first shell and can be derived from either a theoretical calculation or an experimentally determined $\chi(k)$ for which the background is trusted. Optimization with a standard is particularly useful when the scans will later be compared in some way (log-ratios, fitting, etc.) because it gives a consistent, reliable background with a smooth transition from the low-R region into the first shell. Most importantly for optimization using a standard, the resulting background is fairly insensitive to the details of the first peak. Since the standard $\chi(k)$ is used only to get an approximation of the leakage from the first shell, and since the leakage is only a small portion of the first shell, even a crude estimate of the near-neighbor distance and amplitude of χ will make a reasonably good standard for background subtraction.

Because the background removal method makes explicit use of both Fourier conjugate variables k and $2R$, the number and nature of the free variables in the background spline are now well characterized. Since each knot is associated with one degree of freedom, the *maximum* number of knots allowed in the spline is given by[7]

$$N_{\text{knots}} = \frac{2R_{\text{bkg}}\Delta k}{\pi}, \tag{2}$$

where Δk is the k range of useful data and R_{bkg} is the upper limit of the low-R region over which the background is to be fit. Typically, R_{bkg} will be about half the distance of the first shell peak. To minimize R components higher than R_{bkg} in the background, the knots are set to be equally spaced in k space, so that R_{bkg} can be thought of as the Nyquist frequency, above which no signal can be measured. Since Eq. (2) gives an upper limit on N_{knots}, and because the number of knots must be an integer, the actual number of knots used will always be less than or equal to that given by Eq. (2). To be conservative, we use one less knot than the integer part of N_{knots}. (This reduces R_{bkg} to an integer multiple of $\frac{\pi}{2\Delta k}$.) Because of the restrictions now put on the background spline from the information content of $\tilde{\chi}(R)$, the number and abscissas of the knots are now explicitly determined [while the ordinates of the knots are determined by minimizing the difference between data and standard $\tilde{\chi}(R)$ in the low-R region] so that much of the subjectivity of the standard background method is eliminated.

It should be noted here that the standard background removal method approximates this approach by requiring a spline with a limited number of knots in order to prevent any significant part of $\chi(k)$ from being subtracted in the background removal. Many of the difficulties of the standard background method stem directly from trying to fit a function in k space, while the requirements on the function are best expressed in R space. Typically, in fact, backgrounds that are determined in this standard way (i.e., by fitting in k space) are deemed good when the low-R components of $\tilde{\chi}(R)$ are small. The new method, like that of Cook and Sayers,[5] codifies and automates this criterion for a good background.

The data-crossing method discussed above, although it too fits the background in k space, can be seen as a special case of this approach of associating the structural information with χ, and the nonstructural information with the background. Only χ, through variations in partial pair-correlation function, has temperature dependence. The background consists of everything else and so has negligible temperature dependence, and so the two can be separated by comparing the full absorption at different temperatures.

IV. RESULTS AND COMPARISONS

The new background removal technique is applied to the XAFS of the L_{III} edge for pure Pb at 300 K, a system for which the background was determined to 1.5 Å^{-1} by the data-crossing method.[4] The data, which extend to 7.2 Å^{-1}, were optimized at low R by matching as described above to a few slightly different theoretical calculations up to $R_{\text{bkg}} = 1.5$ Å. With $\Delta k = 6.7$ Å^{-1} (the background was fit between $k = 0.5$ Å^{-1} and 7.2 Å^{-1}), Eq. (2) gives $N_{\text{knots}} = 6.4$, while 5 equally spaced knot locations (including end points) were actually used in the background fit. Figure 1 shows the measured $\Delta\mu x(E)$ (after pre-edge background subtraction, but not normalization) and the $\Delta\mu_0 x(E)$ found by fitting the low-R range of $\tilde{\chi}(R)$ to a theoretical calculation of the first shell of Pb at 300 K, and the $\Delta\mu_0 x(E)$ as measured by the data-crossing technique. The inset shows the energy chosen as the Fermi energy, where the first derivative has a local maximum, and the energy of the first data crossing, a conservative estimate for the energy above which the background from this method is reliable. Note that the Fermi energy is not at half the edge step. The width of the total edge step is about 20 eV, significantly larger than the 8-eV lifetime

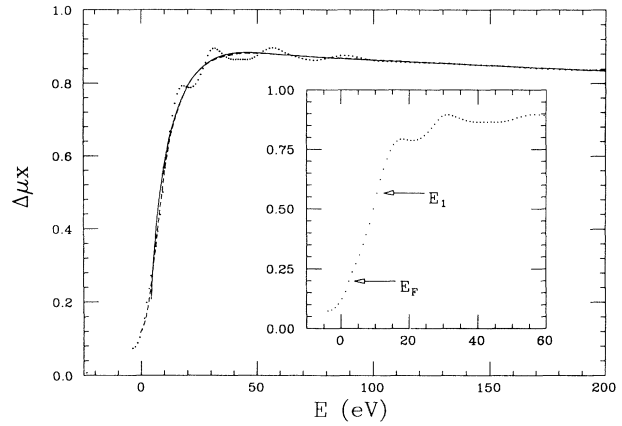

FIG. 1. X-ray absorption spectra for the $L_{\rm III}$ edge of Pb at 300 K (dots). The solid line shows the background from the R-space fitting method, and the dashed line shows the background from the data-crossing method. The inset shows the data points used for the Fermi energy, E_F, and the first reliable data crossing, E_1, above which the background for the data-crossing method is trusted.

broadening,[8] and 3-eV measurement resolution. This indicates that most of the edge step is not a broadened Fermi-energy step. A smaller step with a broadening consistent with the measurement resolution and lifetime broadening is seen at E_F, as shown in Fig. 1. The chosen Fermi energy will be shown below to agree with the calculated Fermi energy.

Figure 2 shows the $k^2\chi(k)$'s and $\tilde{\chi}(R)$ resulting from these background removals. The Fourier transforms were done from $k^2\chi(k)$ to $\tilde{\chi}(R)$ using a Hanning function window,[3] with $k_{\rm min} = 1.25$ Å^{-1}, $k_{\rm max} = 6.25$ Å^{-1}, and $dk = 1.0$ Å^{-1} for both the high and low ends of the k range. The $k^2\chi(k)$'s from the R-space background removal are seen to be very similar to $k^2\chi(k)$ determined by the data-crossing method above 1.5 Å^{-1}, the value of the first reliable data crossing. The difference can be seen to be only at low R. It should be emphasized that these two background removal methods are both more objective than the standard method of least-squares fitting in k space and are independent, giving great confidence in the background for pure Pb above 1.5 Å^{-1} where the absorption is about 70% of the edge jump. Figure 2 shows the results of the background removal using two different standards to optimize the low-R region. The two standards used were both *ab initio* calculations based on the multiple scattering code[9] FEFF version 5.03, using slightly different values for the near-neighbor distance R, overall amplitude S_0^2, and Debye-Waller Factor σ^2. The dashed line shows the background using a standard with $R = 3.479$ Å, $S_0^2 = 0.875$, and $\sigma^2 = 0.0042$ Å^2 . The dots used a standard with $R = 3.51$ Å, $S_0^2 = 1.0$, and σ^2 set to zero. What is important is that, while the theoretical χ's are different from one another and from the resulting χ's extracted from the experimental data, the two extracted χ's from the R-space fitting method are nearly identical. It can therefore be concluded that the details of theory, as long as they are reasonable, do not strongly influence the extracted background. Finally, since this background closely matches that given by the data-crossing method, the R-space fitting method gives the correct background above 1.5 Å^{-1} without the need for a completely reliable theory.

As mentioned above, a severe limitation of the data-crossing technique is the requirement that $\chi(k)$ be dominated by only the first shell. When more than one shell contributes significantly to $\chi(k)$, the data crossings for scans of different temperatures will depend on the temperature-dependent change in relative contributions of the various shells, not the change in the XAFS from an individual shell. In these cases the data crossings will not correspond to the background function. This complication is illustrated in Fig. 3 which shows the measured $\Delta\mu x(E)$ at 30 K and the $\Delta\mu_0 x(E)$ found by both the

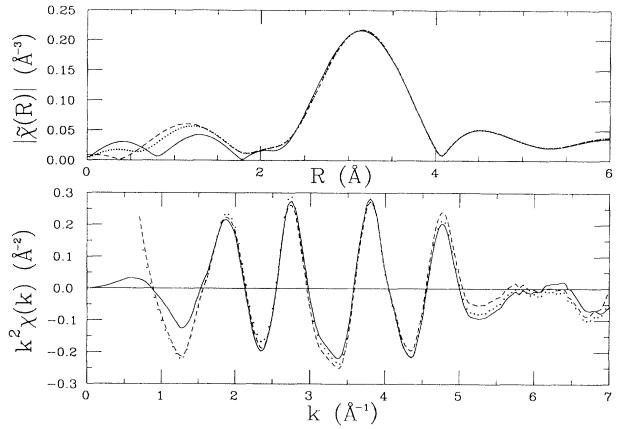

FIG. 2. $k^2\chi(k)$ and $\tilde{\chi}(R)$ for Pb at 300 K using the data-crossing background technique (solid) and the R-space fitting background technique using two slightly different theoretical calculations as the standard (dashed and dots).

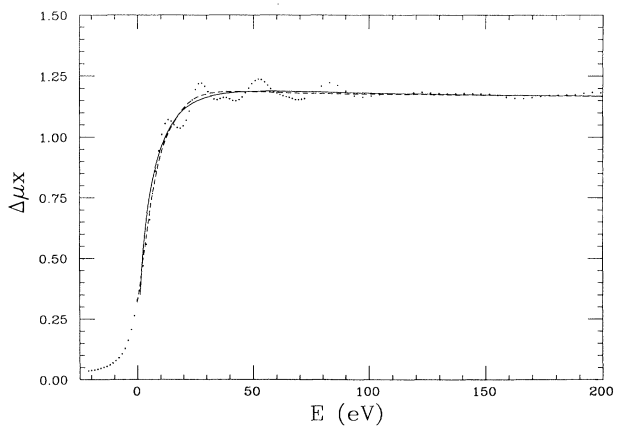

FIG. 3. The low-energy portion of the x-ray absorption spectra for Pb at 30 K (dots). The solid line shows the background from the R-space fitting method, and the dashed line shows the background from the data-crossing method.

data-crossing technique and by fitting the low-R region of $\tilde{\chi}(R)$ to a theoretical calculation of Pb at 30 K. The R-space fitting was done with $R_{\rm bkg} = 1.5$ Å and $\Delta k = 14.5$ Å^{-1} (the background was fit between $k = 0.5$ Å^{-1} and 15.0 Å^{-1}). Equation (2) gives $N_{\rm knots} = 13.8$, and 12 equally spaced knots were used. Note that near the edge the 30-K data shows evidence of significant contributions from higher shells, introducing deviations from a simple sinusoidal variation expected for a single shell, and that, in the same region the two background methods differ. The data-crossing method will fail in this case because of the higher shells involved. Figure 4 shows the resulting $k\chi(k)$ and $\tilde{\chi}(R)$ for the two methods. The Fourier transforms were done from $k\chi(k)$ to $\tilde{\chi}(R)$ using a Hanning function window,[3] with $k_{\rm min} = 1.75$ Å^{-1}, $k_{\rm max} = 13.00$ Å^{-1}, and $dk = 2.0$ Å^{-1} for both the high and low ends of the k range. It is clear from Fig. 4 that the data-crossing background causes large spurious signals at low R which the low-R fitting background is able to remove. Since the same fitting criterion and $R_{\rm bkg}$ (and so the same nominal k spacing of the knots) were used for both the 30-K and 300-K data, the XAFS for Pb at 30 K from the low-R fitting background method will be reliable above 1.5 Å^{-1}.

The reliability of the XAFS of Pb at such low k invites a comparison of the experimental near-edge XAFS to theoretical calculations. The 30-K data is used for this comparison since its $\chi(k)$ is much less attenuated by thermal effects and thus has a better signal-to-noise ratio over a larger k range than does the 300-K data, allowing more accurate determination of the overall EXAFS parameters, such as energy origin and amplitude factor, for the theoretical calculation. Using the low-R fitting background, the experimental $\chi(k)$ above 1.5 Å^{-1} can be compared to theoretical calculations. Figure 4 shows the $k\chi(k)$ for the 30-K data, correctly normalized with the full energy-dependent background function. Since the background drops dramatically at low k, this normalization procedure has the effect of giving $\chi(k)$ a larger amplitude at low k than data normalized to a single number. Although a reasonable fit to higher shells can be obtained for this system when multiple scattering are included, the comparisons with theory discussed here will be limited to the isolated first shell. Figure 5 shows the isolated experimental first shell with three different isolated first shell theoretical calculations[9] using FEFF version 5.03. The first shell was isolated from the $\tilde{\chi}(R)$ shown in Fig. 4 using a Hanning function window,[3] with $R_{\rm min} = 2.60$Å, $R_{\rm max} = 3.85$ Å, $dR = 0.8$ Å.

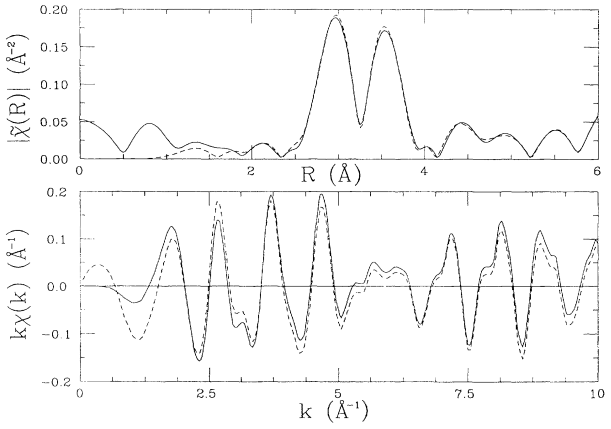

FIG. 4. $k\chi(k)$ and $\tilde{\chi}(R)$ for Pb data at 30 K using the data-crossing background technique (solid) and the R-space fitting background technique (dashed).

Figure 5(a) shows the first shell data and a FEFF calculation using the Hedin-Lundqvist[10] self-energy, near-neighbor distance $R = 3.479$ Å, $S_0^2 = 0.875$, and $\sigma^2 = 0.0042$ Å^2. The energy origin for the data was chosen as E_F, shown in Fig. 3. The energy origin for the FEFF calculation was taken to be 4.2 eV above the muffin-tin zero. (FEFF, using a free-electron model based on its own calculation for the electron density, gives the Fermi energy to be 6.4 eV above the muffin-tin zero. More sophisticated calculations[11] give $E_F = 4.2$ eV, and so this lower value was used instead.) An energy shift of $\Delta E = -0.5$ eV was needed for this theory to best fit the data, well within the uncertainty of the measured Fermi energy for the data, indicating that the Fermi energy is correctly determined for both theory and experiment.

Note that the amplitude of the calculation in Fig. 5(a) is larger than the experiment for k between 2 and 5 Å^{-1}. This discrepancy is due to the simplistic approximation of the plasma loss made in a model self-energy based on a single plasmon pole. However, a significant amount of energy loss occurs through electron-hole excitations below the plasma frequency[12] which are not included in the simple approximation. By adding this additional electron-hole loss term, the calculated amplitude agrees

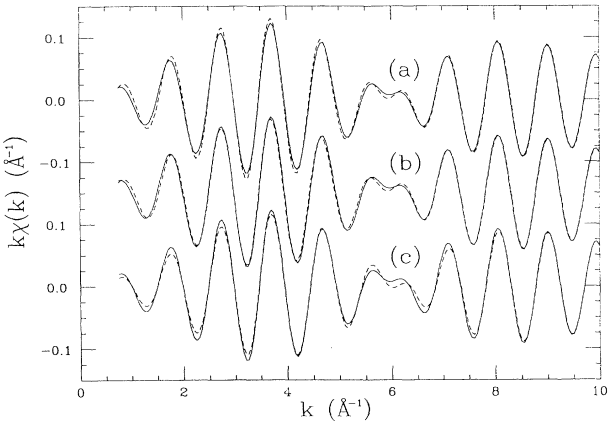

FIG. 5. Comparison of experimental data and calculations using different exchange models for $k\chi(k)$ of the isolated first shell XAFS of Pb at 30 K. (a) Experimental data (solid) and FEFF5.03 using Hedin-Lundqvist exchange, $S_0^2 = 0.875$, $\sigma^2 = 0.0042$ Å^2, and $\Delta E = -0.5$ eV (dashed). (b) Experimental data (solid) and FEFF5.03 using Hedin-Lundqvist exchange with additional plasmon-hole loss term due to Quinn, $S_0^2 = 0.875$, $\sigma^2 = 0.0042$ Å^2, and $\Delta E = -0.5$ eV (dashed). (c) Experimental data (solid) and FEFF5.03 using Dirac-Hara exchange, $R = 3.479$ Å, $S_0^2 = 0.460$, $\sigma^2 = 0.0038$ Å^2, and $\Delta E = +6.5$ eV (dashed).

much better with the data. Figure 5(b) shows the data with a FEFF calculation including the additional loss term calculated using Quinn's approximation,[12] and using the same parameters as for Fig. 5(a). The fit here is quite good over the entire data range. The Debye-Waller factor used for the calculation agrees well with both the value calculated from θ_D and the value[4] extracted from the measured temperature dependence of the XAFS.

When the Hedin-Lundqvist exchange is replaced by a Dirac-Hara exchange[13] in the FEFF calculation, the amplitude is seen to be much too large (Dirac-Hara is a real exchange potential and so allows no loss terms), and the energy origin is quite different than it was for the Hedin-Lundqvist exchange. To make FEFF with a Dirac-Hara model best fit the first shell data, $S_0^2 = 0.460$, $\sigma^2 = 0.0037$ Å^2, and an energy shift of $\Delta E = +6.5$ eV are required. The results of this calculation are shown in Fig. 5(c). The S_0^2 for this calculation is unreasonably small, and the amplitude matches the data more poorly than the calculation with the Hedin-Lundqvist exchange. This indicates that the Hedin-Lundqvist exchange is superior to that of Dirac-Hara for the amplitude calculation, which is not surprising since no losses are allowed in the Dirac-Hara potential. The phase appears to match the data as well as the phase of the calculation with Hedin-Lundqvist exchange, but a large energy shift is required to do this. Because the Fermi energy of the data is thought to be known to within a few eV, this energy shift for Dirac-Hara seems much too large.

For many systems of interest to XAFS problems, the Fermi energy is either difficult to determine from the data or accurate model calculations for the Fermi energy are unavailable. In these cases the energy origin of the data relative to that of a model calculation is completely unknown, and becomes a fit parameter. Since this is often the case, it is important to note that the E_F taken directly from the FEFF calculations (6.4 eV above the muffin-tin level) was found to be 2.7 eV too high when the Hedin-Lundqvist exchange was used, and 4.3 eV too low when the Dirac-Hara exchange was used. Because the more sophisticated calculations for E_F (4.2 eV above the muffin-tin) was used, the Hedin-Lundqvist exchange was found to be only 0.5 eV too high, while the Dirac-Hara was 6.5 eV too low. It must be emphasized, however, that the Fermi level of the data falls between those of the two exchange models using the value for E_F directly from FEFF, and that, when E_F is a fit parameter, the phase shifts from both models give reasonable approximations to the phase shift for Pb data.

V. CONCLUSION

A way to remove the post-edge background for XAFS that is consistent with the carefully and physically determined background from the data crossings of the temperature-dependent data, yet is easier and more general to use, has been presented and demonstrated. The method chooses the background which minimizes the difference of the measured data and a standard (either theoretical or experimental) below the first peak in R-space. The new approach to background removal can be applied to all systems to give results that are reasonable and, based on the results for Pb in this paper, reliable. The technique is especially useful for obtaining near-edge XAFS, which was previously thought too unreliable due to large uncertainties in the background function.

Because such reliable XAFS have been obtained in the low-k region for Pb, tests of and improvements to theoretical calculations in this sensitive region were carried out. It was found that electron-hole losses are significant at energies up to 100 eV above the edge. The Hedin-Lundqvist self-energy for the photoelectron was found to be superior to that of Dirac-Hara for the amplitude for Pb. Since the Fermi energy of Pb can be identified on the absorption edge, the Hedin-Lundqvist exchange also matches the phase shift of the data better than does the Dirac-Hara potential. If the energy origin of the data is taken as a completely free parameter, however, the Dirac-Hara model seems to approximate the phase shift as well as the Hedin-Lundqvist exchange. The superiority of the Hedin-Lundqvist exchange model for the amplitude recommends it for general use. With the additional plasmon loss term for the amplitude and the correct value for the energy origin, the FEFF calculations works quite well for first shell Pb over the XAFS range from 1.5 Å^{-1} to 14.0 Å^{-1}.

ACKNOWLEDGMENTS

The authors thank S. I. Zabinsky for help with FEFF5.03 calculations, and M. X. Qian and B. Ravel for many useful discussions. This research has been supported by DOE Grant No. DE-FG06-90ER45425.

[1] E. A. Stern and S. M. Heald, in *Handbook of Synchrotron Radiation*, edited by E. E. Koch (North-Holland, New York, 1983), Vol. 1, Chap. 10, p. 995.
[2] B. W. Holland, J. B. Pendry, R. B. Pettifer, and J. Bordas, J. Phys. C **11**, 633 (1978).
[3] D. E. Sayers and B. A. Bunker, Chem. Anal. **92**, 211 (1988); in *X-Ray Absorption: Principles, Applications, Techniques of EXAFS, SEXAFS, and XANES*, edited by D. C. Kroningsberger and R. Prins (Wiley, New York, 1988), Chap. 6.
[4] E. A. Stern, P. Livins, and Z. Zhang, Phys. Rev. B **43**, 8850 (1991).
[5] J. W. Cook, Jr. and D. E. Sayers, J. Appl. Phys. **52**, 5924 (1981).
[6] G. Li, F. Bridges, and G. S. Brown, Phys. Rev. Lett. **68**, 1609 (1992).
[7] L. Brillouin, *Science and Information Theory* (Academic, New York, 1962).
[8] O. Keski-Rahkonen and M. O. Krause, At. Data Nucl. Data Tables **14**, 139 (1974).
[9] J. J. Rehr, R. C. Albers, and S. I. Zabinsky, Phys. Rev. Lett. **69**, 3397 (1992); J. J. Rehr and R. C. Albers, Phys. Rev. B **41**, 8139 (1990).
[10] L. Hedin and S. Lundqvist, J. Phys. C **4**, 2064 (1971).
[11] D. A. Papaconstantopoulos, A. D. Zdetsis, and E. N. Economou, Solid State Commun. **27**, 1189 (1978).
[12] J. J. Quinn, Phys. Rev. **126**, 1453 (1962).
[13] P. A. M. Dirac, Proc. Camb. Phil. Soc. **26**, 376 (1930).